# *PF19* encodes the p60 catalytic subunit of katanin and is required for assembly of the flagellar central apparatus in *Chlamydomonas*

**Erin E. Dymek and Elizabeth F. Smith***

Department of Biological Sciences, Dartmouth College, Hanover, NH 03755, USA

*Author for correspondence (elizabeth.f.smith@dartmouth.edu)

*Accepted 12 March 2012*
*Journal of Cell Science 125, 3357–3366*

*doi: 10.1242/jcs.096941*

## Summary

For all eukaryotic cilia the basal bodies provide a template for the assembly of the doublet microtubules, and intraflagellar transport provides a mechanism for transport of axonemal components into the growing cilium. What is not known is how the central pair of microtubules is nucleated or how their associated polypeptides are assembled. Here we report that the *Chlamydomonas pf19* mutation results in a single amino acid change within the p60 catalytic subunit of katanin, and that this mutation prevents microtubule severing activity. The *pf19* mutant has paralyzed flagella that lack the central apparatus. Using a combination of mutant analysis, RNAi-mediated reduction of protein expression and in vitro assays, we demonstrate that the p60 catalytic subunit of the microtubule severing protein katanin is required for central apparatus assembly in *Chlamydomonas*. In addition, we show that in *Chlamydomonas* the microtubule severing activity of p60 katanin is not required for stress-induced deflagellation or cell cycle progression as has been previously reported.

**Key words:** Katanin, Flagella, Cilia, *Chlamydomonas*

## Introduction

Since the discovery of katanin nearly two decades ago, this microtubule severing protein has been implicated in a variety of cellular processes in a diverse range of eukaryotes, from unicellular organisms such as *Chlamydomonas* to humans (McNally and Vale, 1993). Katanin is comprised of two subunits: p60, the catalytic subunit, and p80, a regulatory subunit (Hartman et al., 1998). The p60 subunit is a member of the AAA ATPase family of proteins and possesses microtubule severing activity (Hartman et al., 1998; McNally et al., 2000). In its ATP-bound form katanin assembles into hexameric structures that bind to the microtubule lattice (Hartman et al., 1998; Hartman and Vale, 1999). In one model, interaction of katanin with the C-terminal tails of tubulin results in destabilization of tubulin–tubulin interactions, thus causing the microtubules to sever. The p80 subunit appears to play a role in both targeting p60 and enhancing its microtubule severing activity (McNally et al., 2000). Importantly, katanin is the founding member of a family of microtubule severing proteins that includes spastin, fidgetin, and VPS4 (reviewed in Roll-Mecak and McNally, 2010).

Numerous studies in a variety of cell types have revealed important roles for katanin in organizing centrosomal and/or non-centrosomal microtubule arrays. For example, katanin has been shown to play a role in spindle organization in meiosis (*Caenorhabditis elegans*) and mitosis (several organisms and cell types) (reviewed in Roll-Mecak and McNally, 2010). A recent study in *C. elegans* indicated that the role of katanin in spindle assembly during meiosis was independent of microtubule severing activity (McNally and McNally, 2011). Yet, the microtubule severing activity of katanin contributes to mitotic spindle length scaling among *Xenopus* species (Loughlin et al., 2011). In neurons, katanin appears to regulate axonal growth as well as the length and number of microtubules in mature neurons (Karabay et al., 2004; Yu et al., 2005). In plants, katanin-mediated microtubule severing is required for generating cortical microtubule arrays. Microtubule branches are initiated by gamma-tubulin rings which bind along pre-existing microtubules; katanin-mediated microtubule severing releases these branches allowing for generation of parallel arrays of microtubules (Stoppin-Mellet et al., 2002; Wasteneys, 2002; Stoppin-Mellet et al., 2003; Stoppin-Mellet et al., 2007; Nakamura et al., 2010). More recently, katanin has been shown to act as a depolymerase involved in regulating microtubule dynamics during cell migration (Díaz-Valencia et al., 2011; Zhang et al., 2011).

In the green alga *Chlamydomonas*, several studies have suggested that katanin plays a role in the flagellar autotomy response to stress and in the release of basal bodies from the transition zone prior to mitosis (Lohret et al., 1998; Lohret et al., 1999; Rasi et al., 2009; Parker et al., 2010). We have shown that *Chlamydomonas* mutants with defects in the p80 subunit of katanin have no defects in mitosis or flagellar autotomy; rather, these mutants lack the central pair of microtubules (Dymek et al., 2004). One possibility is that the central pairless phenotype is uniquely associated with defects in the p80 regulatory subunit of katanin. However, this same central pair defect has also been observed in *Tetrahymena* mutants which do not express either subunit of katanin (Sharma et al., 2007). In these studies both the p60 and p80 subunits of katanin are required for assembly of motile, normal-length cilia. Therefore, in at least two protozoa

katanin plays an essential role in cilia biogenesis and specifically in formation of the central pair of microtubules. It is not known if katanin serves a similar role in other ciliated/flagellated cell types.

Unlike the axonemal doublet microtubules that comprise eukaryotic cilia and flagella, the central microtubules are not nucleated from the basal bodies. In conventional transmission electron microscopy the proximal ends of these microtubules (their minus ends) do not appear to have connections to other ciliary or cellular structures. To gain insight into a mechanism for central apparatus assembly, we have undertaken an analysis of the *Chlamydomonas pf19* mutation. *Chlamydomonas pf19* mutants are completely viable with normal cell division and flagellar autotomy responses. However, they have paralyzed flagella that lack the central apparatus. Here we report that *PF19* corresponds to the *KAT1* gene encoding the p60 subunit of katanin and provide evidence that in *Chlamydomonas* katanin plays a critical role in assembly of the central pair of microtubules.

## Results

### *PF19* encodes the p60 subunit of katanin

We previously reported that the *PF15* gene encodes the p80 subunit of katanin (Dymek et al., 2004). Given that both the *pf15* and *pf19* mutants have paralyzed flagella that lack the central apparatus and that the *pf19* mutation maps very close to the *Chlamydomonas KAT1* gene encoding the p60 subunit of katanin (Kathir et al., 2003), we suspected that *pf19* may carry a mutation in the *KAT1* gene. In our initial attempts to sequence the *KAT1* gene amplified from genomic DNA isolated from the *pf19* mutant, we were unable to detect any mutations (Dymek et al., 2004). However, since *Chlamydomonas* DNA is extremely GC rich, we suspected that there may have been technical difficulties in sequencing this region of genomic DNA. Therefore, we recently re-sequenced the *KAT1* gene using different primers and DNA sequencing reagents (see Materials and Methods). We discovered a single mutation, a T to C transition, which converts leucine 277 to serine (Fig. 1A). To ensure that this mutation was not introduced during amplification of the *KAT1* gene, we confirmed the presence of this mutation using multiple primer sets and PCR products were sequenced directly; in addition we isolated RNA from *pf19* cells and used RT-PCR to confirm the presence of the mutation in the *KAT1* transcript produced in these cells. This residue is highly conserved from *Chlamydomonas* to *Arabidopsis* to humans and is within the AAA domain (Fig. 1B). Therefore, we suspected that *pf19*–p60 is non-functional.

To confirm that the central pairless and flagellar paralysis phenotypes are caused by the mutation in *KAT1*, we co-transformed *pf19* cells with a BAC clone containing the full length *KAT1* gene as well as a plasmid with a selectable marker (see Materials and Methods). Clone 27D3 rescues both the motility and structural phenotypes in the *pf19* mutant (data not shown). Out of 96 paromomycin-resistant transformants, five independent isolates were obtained with restored motility. This result is consistent with a co-transformation efficiency of 5% as we and others have previously reported (Tam and Lefebvre, 1993; Smith and Lefebvre, 1996; Smith and Lefebvre, 1997; Smith and Lefebvre, 2000; Dymek et al., 2004). In all of these strains, the presence of the central apparatus was confirmed by western blot using the anti-PF20 antibody (Smith and Lefebvre, 1997) (data not shown). We then subcloned the *KAT1* gene from BAC 27D3. This 6kb subclone (pBCp60) includes ~600 bp upstream of the translational Start and ~1200 bp downstream of the translational Stop (see supplementary material Fig. S1 for details). The coding sequence of katanin p60 is the only coding sequence predicted within this 6 kb span of genomic DNA. The pBCp60 plasmid rescues both the motility and structural defects in the *pf19* mutant upon transformation (co-transformation efficiency of 5%). These results indicate that *PF19* corresponds to *KAT1* encoding the p60 subunit of katanin and that the *pf19* mutation is recessive.

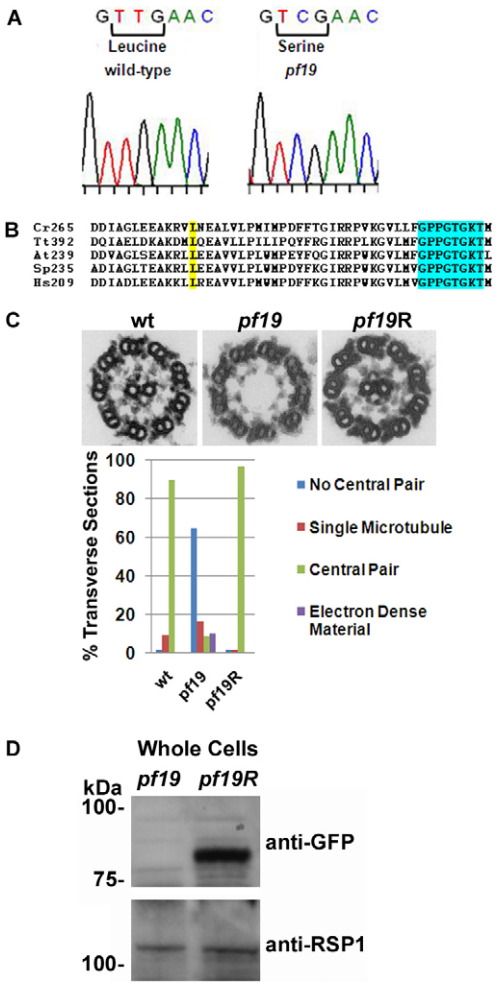


**Fig. 1. The *pf19* gene sequence and *pf19* mutant rescue.** (**A**) Sequencing data of the *KAT1* gene reveals a T to C transition, which converts leucine 277 to serine. (**B**) Amino acid sequences of a portion of the p60 AAA domain from *Chlamydomonas reinhardtii* (Cr), *Tetrahymena thermophila* (Tt), *Arabidopsis thaliana* (At), sea urchin *Strongylocentrotus purpuratus* (Sp) and humans (Hs). This leucine (yellow highlight) is highly conserved in p60 from *Chlamydomonas* to mammals and is within the AAA domain, only 28 amino acids upstream from the Walker A nucleotide binding motif (turquoise highlight). (**C**) Electron micrographs of transverse sections of axonemes isolated from wild-type, *pf19* and *pf19*R (*pf19* cells rescued with the GFP-pBCp60 construct) cells. The histogram shows the number of central pair microtubules present in transverse sections of WT, *pf19* and *pf19R* transverse sections ($n>75$ sections for each strain). The central apparatus is missing from *pf19* axonemes and is restored in axonemes from *pf19* cells that were transformed with GFP-pBCp60. (**D**) In western blots, anti-GFP antibodies recognize a band of ~85 kDa in the *pf19*R whole cell lane, which is not in the *pf19* lane. Blots were probed with antibodies generated against radial spoke protein RSP1 as a loading control.

In an effort to localize p60 we generated a plasmid construct encoding p60 fused with a GFP tag (see Materials and Methods and supplementary material Fig. S1). We engineered the p60–GFP construct to express GFP at the amino terminus of the p60 protein. This construct rescued motility and central apparatus assembly upon transformation into *pf19* mutant cells (co-transformation efficiency of 5%, Fig. 1C). For axonemes prepared from *pf19* cells, 8.7% of transverse sections have a central apparatus. In *pf19* mutants rescued with the GFP–pBCp60 plasmid, greater than 90% of transverse sections have a central apparatus, comparable to wild type (Fig. 1C). Expression of the GFP construct was confirmed by western blots of cell extracts isolated from rescued strains (Fig. 1D). We could not detect p60–GFP in isolated flagella indicating that either all p60–GFP is located in the cell body or that the amount in flagella is below the limit of detection by western blot. Attempts to localize GFP–p60 by fluorescence microscopy were not successful. These experiments included visualizing GFP directly as well as using anti-GFP antibodies and fluorescently labeled secondary antibodies. Based on western blots as well other studies of p60, we suspect that p60 is not an abundant protein. It is also possible that the GFP is not accessible to the anti-GFP antibodies.

As a second method to potentially localize p60 in wild-type cells and to determine if p60 protein is expressed in the *pf19* mutant, we obtained anti-p60 katanin antibodies provided by the Quarmby lab (Rasi et al., 2009). The anti-p60 serum did not recognize the tagged p60–GFP protein in whole cell extracts (supplementary material Fig. S2B). Based on results shown in supplementary material Fig. S2A we concluded that this antibody is not of sufficiently high titer or specificity to recognize p60 in cell extracts. Therefore, we did not use this p60 antibody in any additional studies. To date, no commercially available antibodies recognize *Chlamydomonas* p60.

### The *pf19*-p60 subunit of katanin lacks microtubule severing activity

One possibility is that the central pairless phenotype of the *pf19* mutation is due to an incomplete loss of p60 function. To determine if the *pf19*-p60 protein retains severing activity, we obtained cDNAs encoding either wild-type p60 or *pf19*-p60 and expressed either of these two proteins in bacteria. For both wild-type p60 and *pf19*-p60, the proteins were expressed as fusions with a GST tag at the amino terminus of the protein (see Materials and Methods and supplementary material Fig. S2A). Importantly, to obtain full length protein that is soluble under non-denaturing conditions, these proteins were expressed in Rosetta-gami bacteria (Novagen) and induction of expression was carefully controlled (see Materials and Methods). The expressed protein was affinity purified and then assessed for microtubule severing activity using microtubules assembled in vitro and dark-field microscopy (see Materials and Methods).

In the severing assay, microtubules are added to a flow-through chamber constructed as described in the Materials and Methods. Microtubules that do not adhere to the slide are washed through the chamber. In control experiments with no added expressed p60 protein, flow of buffer through the chamber results in the detachment of a certain small percentage of microtubules from the coated slide which then flow out of the chamber. This loss of microtubules was quantified from multiple control experiments using ImageJ (see Materials and Methods) as a 16% reduction in microtubule density. In stark contrast, 20 minutes after bacterially expressed *Chlamydomonas* wild-type p60 and ATP are added to the chamber, the density of microtubules was reduced by 40% (Fig. 2). This significant reduction ($P=0.0005$, Student's *t*-test) in microtubule density was not seen in experiments using expressed *pf19*-p60. In experiments with mutant protein, the small reduction in microtubule density observed 20 minutes after addition of the *pf19*-p60 protein (~16%) was not significantly different ($P=0.98$, Student's *t*-test) from control experiments with no added p60 protein. The simplest interpretation is that the *pf19* mutation abolishes microtubule severing activity of the p60 protein.

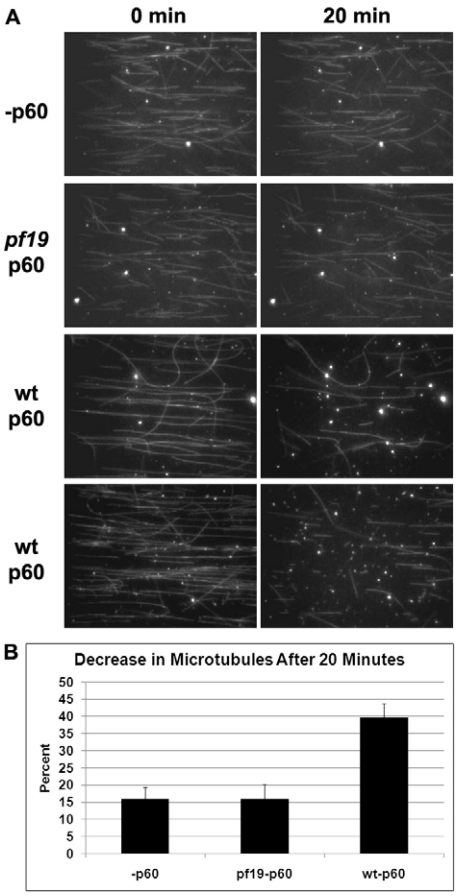


**Fig. 2. Microtubule severing with wild-type or *pf19* p60-GST.** (**A**) Images of microtubules taken at 0 and 20 minutes after exposure to buffer alone (−p60), *pf19* p60-GST or wild-type p60-GST. The images of both −p60 and *pf19*-p60 show a small reduction in microtubules; however, the wt-p60 images show a significantly greater microtubule loss (quantified in B). This loss in the wt-p60 images is due to severed pieces of microtubules being washed out of view, because they are not attached to the rest of the microtubule adhered to the slide. (**B**) Quantification of the loss of microtubules between 0 and 20 minutes, determined using ImageJ. At least 10 sets of images for each group (−60, *pf19*-p60 and wt-p60) were analyzed. The Y-axis represents the percentage decrease in microtubules 20 minutes after the addition of buffer alone or p60. The *pf19*-p60 samples had the same amount of microtubule loss as the –p60 control samples (16%, $P=0.98$). However, wt-p60 samples had significantly more microtubule loss (40%, $P=0.0005$). These results reveal that wild-type *Chlamydomonas* p60 severs microtubules in vitro, whereas *pf19*-p60 does not possess microtubule severing activity.

### Knockdown of *KAT1* expression in *Chlamydomonas* results in paralyzed flagella that lack the central apparatus

To explore the difference between the phenotype for the *pf19* mutant (this study) and p60 mutants generated by RNAi-mediated reduction of *KAT1* expression (Rasi et al., 2009), we used an artificial microRNA (amiRNA) approach (Molnar et al., 2009; Zhao et al., 2009) to reduce *KAT1* expression. This technique takes advantage of the cell's own microRNAs that function to regulate endogenous gene expression. Two different gene-specific amiRNA vectors targeting *KAT1* were constructed as described previously (Molnar et al., 2009) and in the Materials and Methods, and these were separately transformed into wild-type *Chlamydomonas* cells (Kindle, 1990). After selection of transformants on paromomycin, colonies were picked into liquid media and screened for abnormal cell division or swimming phenotypes. A total of 2,112 transformants were picked into liquid media from three independent transformations for each construct. Since no anti-p60 antibodies are available for *Chlamydomonas* (described above), we continued our screen based on the known *pf19* phenotype, paralyzed flagella which lack the central apparatus.

Of the transformants picked into liquid media, 90 strains showed motility defects. This is not uncommon since integration of the transforming plasmid may generate a mutant phenotype (Tam and Lefebvre, 1993). These strains were then screened for central apparatus defects by western blot using antibodies generated against the central pair protein, PF20. Of these strains, three (A5, G3, H6) had reduced PF20 protein in isolated axonemes and were chosen for additional studies. All three of these transformants were generated using the same amiRNA construct targeting nucleotides 79–98 of the *KAT1* coding sequence. Importantly, this region of the *KAT1* gene is unique and shares no similarity with other members of the microtubule severing family of proteins.

Based on western blots of axonemes isolated from these three strains, the central pair protein PF20 is reduced to 50% (A5) or to nearly 0% (H6) of wild-type levels (Fig. 3A). Thin section transmission electron microscopy revealed that these amiRNA mutants lacked the central apparatus (Fig. 3B). The numbers of axoneme transverse sections which lack the central apparatus or in which only electron dense material was found are quantified in (Fig. 3C). As predicted by western blots, approximately 50% of axonemes retained the central apparatus in transverse sections of A5 axonemes. However, in both G3 and H6, only about 10% of transverse sections of axonemes retained the central pair of microtubules. By comparison, in axonemes prepared from *pf19* cells, 8.7% of transverse sections have a central apparatus.

To confirm that these strains have reduced levels of the *KAT1* transcript, we isolated RNA from each amiRNA strain, as well as wild-type and *pf19* cells, and examined transcript levels by northern blot analysis and subsequent densitometry (Fig. 4A). RNA was isolated both before and 45 minutes post-deflagellation. The *pf19* mutant produces a *KAT1* transcript as expected since *pf19* is a missense mutation. Northern blots prepared from cells prior to deflagellation revealed that the *KAT1* transcript was reduced to between 40% and 60% of wild-type levels. Northern blots prepared from cells 45 minutes following deflagellation revealed that the *KAT1* transcript was reduced to between 30% and 80% of wild-type levels. In the absence of antibodies to detect p60 in whole cell extracts, we could not assess the relationship between transcript levels and p60 protein levels.

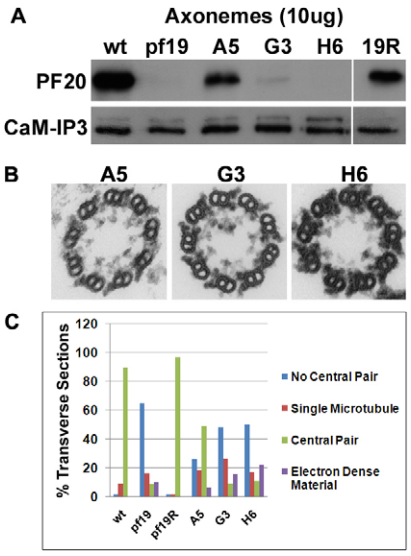


**Fig. 3. Analysis of p60 amiRNA mutants.** (**A**) Western blots of axonemes isolated from WT, *pf19*, *pf19* cells rescued with the WT *KAT1* gene (19R) and three p60 amiRNA mutants (A5, G3, H6). Blots were probed with antibodies to a central pair marker (PF20) and antibodies to CaM-IP3 as a loading control. PF20 is missing or reduced in *pf19*, A5, G3 and H6. G3 and H6 have significantly less PF20 than A5. (**B**) Electron micrographs of transverse sections of axonemes from p60 amiRNA mutants showing that the central apparatus is lacking in these mutants. (**C**) Histogram of the number of central pair microtubules present in transverse sections of WT, *pf19, pf19*Rand p60 amiRNA mutant (A5, G3, H6) axonemes ($n>75$ transverse sections for each strain). The majority of sections for wild-type and *pf19*R axonemes have two central microtubules. For A5, ~50% of transverse sections have both central microtubules. Only ~10% of transverse sections for G3 and H6 have both central microtubules, similar to *pf19* axonemes. Data from Fig. 1C has been included for comparison.

To determine if these three transformants represent independent transformation events, we tested for restriction length polymorphisms (RFLPs) at the integration site. Southern blots of DNA isolated from the three amiRNA strains with reduced *KAT1* expression and probed with the vector sequence from the plasmid revealed RFLPs in these three strains (Fig. 4B). These results indicate the plasmid integrated into different regions of the genome for each strain and demonstrated that the three strains represent independent isolates.

It is possible that since we screened for transformants with motility and central apparatus defects, we isolated insertional mutants in which the amiRNA construct integrated into a gene required for central apparatus assembly. These transformants were originally identified for their absence of PF20 protein in isolated axonemes. The only insertional mutants isolated to date which lack PF20 are the central pair mutants *pf20* and *pf15*. The only other central apparatus defective mutants available which lack PF20 are *pf18* and *pf19*; to date, no insertional alleles of these mutations have been reported. To determine whether the *KAT1* (*PF19*), *PF20* or *PF15* genes were affected by the integrated plasmid in the amiRNA strains, we probed southern blots of genomic DNA isolated from each strain with the full length *KAT1*, *PF15* and *PF20* genes. No RFLPs were observed for any of these genes (data not shown). Therefore, the amiRNA

construct did not disrupt any of these genes. As an important note, no central pairless mutants have been reported in *Chlamydomonas* in which 50% of axoneme transverse sections lack the central apparatus, such as we see for strain A5.

### Flagellar excision and cell growth/division are wild type for both the *pf19* mutant and strains with reduced expression of *KAT1*

To determine if p60 katanin plays a role in flagellar excision, we performed deflagellation experiments in response to pH shock.

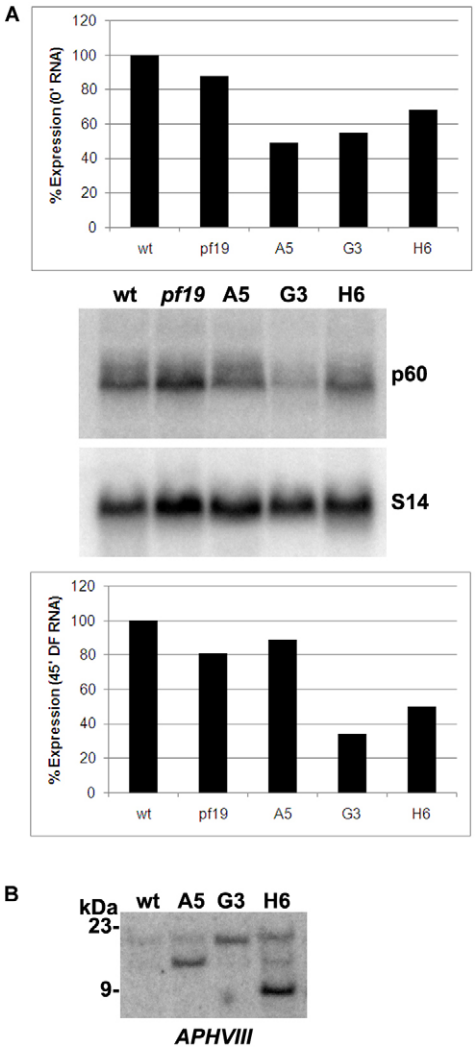


**Fig. 4. Northern and Southern blot analyses of p60 amiRNA mutants.** (**A**) Histograms showing p60 transcript levels before and after deflagellation. 10 µg poly(A)$^+$ RNA were loaded onto gels and the resulting blots were probed with full-length *KAT1*cDNA and, the ribosomal *S14* gene as a loading control. The top histogram shows mRNA levels before deflagellation. The middle panels are northern blots showing RNA levels before deflagellation. The lower histogram shows mRNA levels 45 minutes after deflagellation. *KAT1* transcript levels were normalized using the S14 loading control (see Materials and Methods). Blots for both before and after deflagellation were repeated for a minimum of three different experiments and consistent results were obtained. (**B**) Southern blot of 5 µg DNA digested with KpnI. Blots were probed with the *APHVIII* gene to identify the integrated plasmid. RFLPs are present in the three mutants, indicating the *APHVIII* gene inserted into a different site in the genome for each mutant.

For all three amiRNA strains as well as the original *pf19* mutant, 100% of the cells deflagellate in response to acidic pH (Fig. 5A). As is true for wild-type cells, these strains immediately shed their flagella when the pH of the media is dropped to pH4.5. We have also constructed a *pf15pf19* double mutant which carries mutations in both the regulatory p80 and catalytic p60 subunits of katanin. This *pf15pf19* strain, like both parental strains, has paralyzed flagella which lack the central apparatus (not shown). This double mutant is also wild type for the flagellar excision response (Fig. 5A).

Rasi et al. proposed that the microtubule-severing function of katanin is required not only for flagellar autotomy to sever axonemal microtubules distal to the transition zone, but also to release the basal bodies from the transition zone so that as centrioles, they may participate in spindle positioning during mitosis (Rasi et al., 2009). This severing activity would occur proximal to the transition zone. Parker et al. recently demonstrated

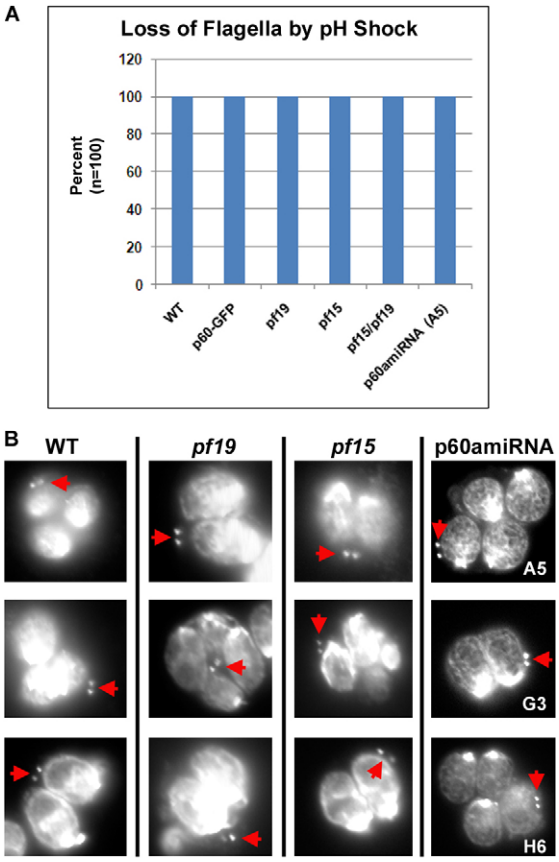


**Fig. 5. Flagellar excision of WT and p60 mutants.** (**A**) Flagellar autotomy response WT and p60 mutants. Deflagellation was induced by lowering the pH of the medium to 4.5. For all strains, pH shock induces flagellar autotomy in 100% of cells. (**B**) Dividing wild-type, *pf19* and *pf15* cells as well as p60amiRNA strains (A5, G3, and H6) were labeled with anti-acetylated α-tubulin. Three images of each cell type are shown for WT, *pf19* and *pf15*. One representative image is shown of each p60 amiRNA strain. The cells had divided at least once and were still encased in the mother cell wall. Red arrowheads point to the flagellar remnants in each image. The presence of these remnants indicates that in cells with reduced expression of *KAT1* or with mutations in either the p60 (*pf19*) or p80 (*pf15*) subunit of katanin microtubules are severed between the basal bodies and flagellar transition zone.

that this severing activity occurs following flagellar resorption and prior to cell division (Parker et al., 2010). Using anti-acetylated α-tubulin antibodies, immunofluorescence microscopy revealed the presence of two bright dots near recently divided cells, but which had not yet hatched from the mother cell wall. These dots were presumed to be the flagellar remnants left by excision from the basal bodies. Parker et al. then showed by electron microscopy that these bright dots are in fact the flagellar remnants that result from this excision event. To test whether KAT1 is required for excision between the basal bodies and the transition zone, we tested for the presence of flagellar remnants in newly divided wild-type, p60 amiRNA strains, *pf15*, and *pf19* cells using anti-acetylated α-tubulin antibodies (Fig. 5B). In all cases the two dots which correspond to flagellar remnants were present. Therefore, excision proximal to the transition zone appears to be wild-type in p60 amiRNA strains as well as for *pf19* and *pf15* cells.

We also assessed whether *pf19* or any of the amiRNA strains exhibited cell division defects by assessing culture density over several days. Cultures were inoculated with the same number of cells and then cells were counted over the course of several days. We could discern no significant differences between the amiRNA strains or the *pf19* mutant compared to wild-type cells (Fig. 6). We also did not observe any clumpy phenotypes or cells with apparent cell division defects. Therefore, neither the *pf19* mutation nor the knockdown of *KAT1* expression results in defects in cell division or loss of viability. The double mutant *pf15pf19* also has no cell cycle defects (not shown).

## Discussion

For motile eukaryotic cilia and flagella the central apparatus plays a crucial role in generating wild-type waveforms and beat frequency. While important and significant advances have recently been made in the field of ciliogenesis, we still do not know how the central pair of microtubules and associated projections are assembled in the axoneme. In *Chlamydomonas* several gene products have been identified which affect assembly/stability of specific projections on the central tubules; PF6 (Dutcher et al., 1984), Cpc1 (Mitchell and Sale, 1999), Hydin (Lechtreck and Witman, 2007), and FAP74 (DiPetrillo and Smith, 2010). However, mutations resulting in a complete failure of the central tubules to assemble are arguably the most likely to provide important information about a mechanism for the genesis of the central apparatus.

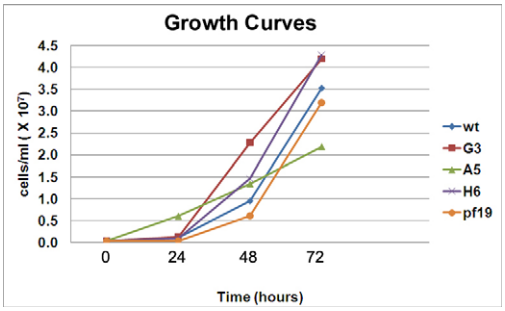


**Fig. 6. Cell growth curves for WT and p60 mutants.** WT, *pf19* and p60 amiRNA mutant cells were counted, resuspended at an equal density, and grown for 3 days. Samples of cells were taken every 24 hours, counted and plotted. There was no significant difference in cell growth between WT, *pf19* and the p60 amiRNA mutants.

In *Chlamydomonas*, only four mutations have been reported that result in a central pairless phenotype (*pf15, pf18, pf19*, and *pf20*), all of which have paralyzed flagella (Adams et al., 1981; Dutcher et al., 1984). Of these mutations the sequence and localization of only the *PF15* and *PF20* gene products has been reported (Smith and Lefebvre, 1997; Dymek et al., 2004). The amino acid sequence of PF20 did not provide significant clues into the mechanism of central pair assembly. However, *PF15* encodes the *Chlamydomonas* homologue of katanin p80. Data reported in this study reveal that the *pf19* mutation resides within the *KAT1* gene encoding the p60 subunit of katanin. These *Chlamydomonas* mutants imply that katanin plays a critical role in central apparatus assembly.

### The *pf19* mutation is within the *KAT1* gene encoding katanin p60 and abolishes p60 microtubule severing activity

The conclusion that *PF19* corresponds to *KAT1* is based on discovery of a T to C transition in the *KAT1* coding sequence, which converts leucine 277 to serine. This mutation was observed using multiple, different, primer pairs for amplification of genomic DNA as well as in cDNA generated from transcripts isolated from the *pf19* mutant; furthermore, this was the only mutation observed for the entire coding sequence. Therefore, it is highly unlikely this same mutation occurred multiple times during PCR amplification. In addition, both the motility and central apparatus defects in the *pf19* mutant were rescued upon transformation of *pf19* cells with a plasmid containing only the *KAT1* coding sequence. Therefore, wild-type *PF19* corresponds to *KAT1*.

Our data argue that the *pf19* mutation L277S renders p60 nonfunctional. L277 is highly conserved in p60 from *Chlamydomonas* to mammals and is within the AAA domain, only 28 amino acids upstream from the Walker A nucleotide binding motif. This AAA domain is required for nucleotide binding, oligomerization, nucleotide hydrolysis, and microtubule severing activity (Hartman and Vale, 1999). In addition, we have demonstrated using in vitro assays that the expressed *pf19*-p60 protein cannot sever microtubules. It is possible that the *pf19*-p60 protein is nonfunctional when expressed in bacteria. However, a wild-type construct has severing activity when generated, expressed and purified by the same methods. Therefore, it is highly unlikely that a technical problem occurred for the *pf19*-p60 construct that was not observed for wild-type p60.

### Is katanin required for flagellar excision in *Chlamydomonas*?

It has been proposed that katanin is involved in microtubule severing at a position distal to the transition zone during stress-induced flagellar excision (Lohret et al., 1998; Lohret et al., 1999). Our studies indicate that the microtubule severing activity of katanin is not required for flagellar autotomy. When expressed in vitro, the *pf19*-p60 protein does not have microtubule severing activity. Yet, the *pf19* mutant, like the *pf15* mutant in which katanin p80 is mutated, retains the flagellar excision response to pH shock. A *pf15pf19* double mutant is also wild type for the deflagellation response. We obtained the same phenotype when we reduced *KAT1* expression using an amiRNA approach. These strains have central pairless flagella with no defects in flagellar autotomy. Collectively, these data strongly support the conclusion that the microtubule severing activity of p60 is not

required for deflagellation and appear to be at odds with data previously published by others (Lohret et al., 1998; Lohret et al., 1999). These studies reported that an antibody generated against human katanin prevented flagellar excision. It is not clear why these particular antibodies prevent flagellar excision. There are two other potential microtubule severing proteins in *Chlamydomonas*, Kat2 (C_620017) and a predicted spastin-like protein. It is possible that the anti-human katanin antibodies recognize one of these potential severing enzymes in *Chlamydomonas* and that one of them is required for flagellar excision. Previous studies have indicated that centrin plays a role in the flagellar autotomy response (Sanders and Salisbury, 1994). Cells with mutations in centrin do not excise their flagella in response to low pH and antibodies generated against centrin also block flagellar excision.

It has also been proposed that katanin is required to sever axonemal microtubules proximal to the transition zone and distal to the basal bodies (Parker et al., 2010; Rasi et al., 2009). This activity results in the appearance of flagellar remnants that can be detected by immunofluorescence and electron microscopy (Parker et al., 2010). Since we show here that these remnants are present in the p60 amiRNA strains and *pf19* mutant, and that the *pf19* mutation abolishes microtubule severing activity, we conclude that microtubule severing by p60 is not the source, or at least not the sole source, of this severing activity.

### Is katanin essential in *Chlamydomonas*?

Rasi et al. recently reported that katanin function is essential in *Chlamydomonas* (Rasi et al., 2009). This conclusion was based in part on the observation that genetic screens failed to yield mutants in the catalytic subunit of katanin and in part from their efforts to knock down *KAT1* expression using an RNAi approach. In these experiments they were unable to obtain stable knockdown of *KAT1* expression in wild-type cells, yet *KAT1* expression was reduced in strains which lacked flagella. They concluded that reduction of *KAT1* expression is lethal in wild-type flagellated cells, but that katanin is not essential for cells which lack flagella. Their working hypothesis is that the microtubule severing function of katanin is required to release the basal bodies from the transition zone to participate in spindle positioning in mitosis. This severing activity occurs between the basal body and transition zone (see also Parker et al., 2010). In cells lacking flagella, katanin would presumably not be required, although admittedly, the flagella-less cells used in their study still possess basal body attachments to the transition zone (in contradiction to their working model). As noted above, in this study we have shown that flagellar remnants that result from microtubule severing proximal to the transition zone are present in the *pf19* and p60 amiRNA mutants. Therefore, this severing is likely not the result of p60 function.

The *pf15, pf19*, and *pf15pf19* double mutants are all viable and show no sign of cell cycle defects. While these mutations are not null mutations, we have shown that the *pf19* mutation abolishes microtubule severing activity. Therefore, the microtubule severing activity of katanin is not required for cell cycle progression. Our *KAT1* knockdown strains are also viable with no cell cycle defects. One explanation for the difference in phenotype for the *KAT1* knockdown strains produced by Rasi et al. compared to those reported here is the difference in method for reducing transcript levels (Rasi et al., 2009). We have tried numerous RNAi methods for reducing protein expression (unpublished results), and all of these methods produced a significant number of off-target effects. We have found that the amiRNA approach of Molnar et al. (Molnar et al., 2009) generates strains with stable knockdown of protein expression without these off-target effects (reviewed in DiPetrillo and Smith, 2010; Dymek et al., 2011; and unpublished observations for three additional axonemal proteins). It is also possible the antibody used by Rasi and colleagues (Rasi et al., 2009) for screening knockdown of expression is not specific (supplementary material Fig. S2).

Particularly noteworthy, a mutation which abolishes severing activity in the catalytic subunit of katanin (MEI-1) in *C. elegans* does not affect spindle assembly (McNally and McNally, 2011), whereas a null mutation causes defects in female meiotic spindle assembly (Mains et al., 1990). These authors propose a role for katanin in spindle assembly that does not require microtubule severing activity. This conclusion is in agreement with the data reported here that show p60 microtubule severing activity is not required for cell division in *Chlamydomonas*. Until a null mutation in *KAT1* is identified, we cannot rule out the possibility that some additional function of katanin p60 unrelated to microtubule severing is required for cell cycle progression.

In addressing the question of whether p60 function is essential in *Chlamydomonas* it is important to recognize that there are two other potential microtubule severing proteins in *Chlamydomonas*, Kat2 (C_620017) and a predicted spastin-like protein. One possibility is that in the absence of p60, either of these two severing proteins may substitute for a specific p60 function, with the exception of central apparatus assembly. In *Arabidopsis*, the katanin most related in amino acid sequence to *Chlamydomonas* katanin does not appear to be essential. Multiple mutations have been isolated in the *Arabidopsis KAT1* gene and all of these mutants are viable (Bichet et al., 2001; Burk et al., 2001; Webb et al., 2002; Bouquin et al., 2003; Nagawa et al., 2006). Moreover, Nagawa et al. generated a katanin mutant using a gene trapping technique; in this case the gene trap tag inserted in the second exon of the katanin coding sequence, most likely generating a null mutant (Nagawa et al., 2006). In *Tetrahymena*, null *KAT1* mutants complete nuclear division but have defects in cytokinesis, forming chains of attached cells (Sharma et al., 2007). For these cells, cilia assemble which are shorter than normal and which lack the central apparatus. Also in *Tetrahymena*, Sharma et al. demonstrated that heterokaryon progeny cells lacking either KAT2 or SPA1 (spastin) had a normal cell morphology and gave rise to clones with normal vegetative growth rates (Sharma et al., 2007). In *Trypanosoma bruceii*, knock down of *KAT1* expression does not result in defects in either nuclear or cell division (Casanova et al., 2009); however, it was not reported in these studies if the flagellum retained wild-type structures.

### The role of katanin in central apparatus assembly

Based on our finding that mutations within either subunit of katanin result in paralyzed, central pairless flagella, it is clear that katanin function is required for assembly of the central apparatus in *Chlamydomonas*. The question now is, what is the mechanism by which microtubule severing activity contributes to the genesis of the central pair of microtubules? Particularly relevant to this question are studies in plant cells and in neurons. Comparisons have been made between the genesis of the parallel cortical array of microtubules in plants and those found in the axons of neurons

(Gardiner and Marc, 2011). In both cell types, katanin appears to sever microtubules to produce shorter pieces which then translocate. In neurons, the severed microtubules translocate into the growing axon (Ahmad et al., 1999; Karabay et al., 2004; Yu et al., 2005; Yu et al., 2008; Baas and Sudo, 2010). In plant γ-tubulin rings bind to the side of existing microtubules to form branches, these microtubule branches are severed by katanin, which then form parallel microtubule arrays (Stoppin-Mellet et al., 2002; Wasteneys, 2002; Stoppin-Mellet et al., 2003; Stoppin-Mellet et al., 2007; Nakamura et al., 2010). Presumably the severed microtubules are stabilized by post-translational modifications or microtubule binding proteins to avoid complete disassembly from newly freed minus ends. The net result in both cases is the rapid reorganization of non-centrosomal microtubule arrays.

Perhaps central microtubule assembly in cilia is analogous to the assembly of these non-centrosomal microtubule arrays. In trypanosomes, McKean et al., 2003 have demonstrated that γ tubulin is specifically required for central apparatus assembly (McKean et al., 2003). In *Chlamydomonas*, γ tubulin has been localized to the transition zone (Silflow et al., 1999) where central apparatus assembly is believed to initiate. Based on work in *Arabadopsis* combined with studies in *Chlamydomonas*, trypanosomes, *Tetrahymena* and neurons, it is tempting to propose a model of central microtubule assembly where γ tubulin initiates microtubule growth from the lateral surface of an existing microtubule; katanin would then sever the new microtubules to form the central pair in the center of the axoneme. One prediction of this model in light of our results is that the *pf15* and *pf19* mutants may still have un-severed, nascent central tubules located near the base of the flagellum. To our knowledge there has not been a complete structural characterization of this region for either of these mutants.

Future studies of katanin function in *Chlamydomonas* and its role in central apparatus assembly will require additional information about the localization of both the p80 and p60 subunits during flagellar assembly as well as the identification of potential katanin interacting proteins. In addition, it will be important to know how this activity is coordinated with post-translational modifications known to occur on axonemal microtubules (reviewed by Gaertig and Wloga, 2008) and which may affect katanin activity, for example (Sudo and Baas, 2010). Finally, it would be of great interest to know in what gene the *pf18* mutation resides. This is the only mutation which yields a central pairless phenotype and for which we have not yet identified the mutated gene. Most likely identification of the wild-type *PF18* gene and gene product will reveal additional insights into central apparatus assembly.

## Materials and Methods

### Strains and cell culture

*Chlamydomonas reinhardtii* strain A54-e18 (*nit1-1, ac17, sr1*,mt+) has wild-type motility and was obtained from Paul Lefebvre (University of Minnesota, St Paul, MN). The *pf19* and *pf15* strains were obtained from the *Chlamydomonas* Genetics Center (University of Minnesota, St. Paul, MN). A *pf15pf19* double mutant strain was isolated from non-parental ditype tetrads resulting from crosses using *pf19* and an insertional allele of *pf15* (Dymek et al., 2004). Cells were grown in constant light in TAP media (Gorman and Levine, 1965). Generation of the *pf19* rescue strains and p60 amiRNA strains is described below.

### Cloning the *PF19* gene and cDNA expression

All cloning procedures are described in supplementary material Fig. S1; primers are listed in supplementary material Table S1. The *PF19* gene was subcloned from BAC 27D3 (the BAC library (CRCCBa) was constructed by Paul Lefebvre and purchased from CUGI (Clemson University Genomics Institute). A 4 kb ClaI–ClaI fragment and a 2 kb ClaI–BamHI fragment were ligated into pBluescript (Stratagene) digested with ClaI and BamHI (final clone consists of −542 bp to +1248 bp of the *KAT1* gene). This clone, pBCp60, was used to construct a GFP–p60 clone. Our goal was to engineer the GFP coding sequence at the most 5′ location in the p60 gene (supplementary material Fig. S1). To do this, we first used a series of PCR reactions to engineer convenient restriction sites for cloning the gene encoding GFP into the 5′ end of the gene encoding p60. A first set of primers engineered an XhoI site 1022 bp upstream of the translational start site and an EcoRI site immediately upstream of the start site (primers P60Xho and P60NEco). These primers were used to amplify the 5′ end of the gene by PCR using BAC 27D3 as a template. The resulting product (PCR1) was cloned into pCR2.1 (Invitrogen). A second set of primers engineered an XbaI site immediately downstream of the start site and a NotI site just 3′ to the endogenous MluI site (primers P60NXba and P60MluNotI). These primers were used to amplify this region by PCR using pBCp60 as a template. The amplified product (PCR2) was cloned into pCR2.1. A third set of primers was used to engineer an EcoRI site 3′ of the GFP start and an XbaI site just 5′ of the GFP stop (primers P60GFPNEco and P60GFPXba) using pCR-GFP (generously provided by Karl Lechtreck) as a template. The amplified product, PCR3, was cloned into pCR2.1. For all plasmids, PCR1, PCR2, and PCR3, the PCR product inserts were excised using the restriction enzymes corresponding to the engineered sites and gel purified. pBluescript was digested with XhoI and NotI, and in a trimolecular reaction, PCR1, 2 and 3 were ligated together into the digested vector; the resulting plasmid was named 5′GFP-p60pBlue. This ligation created two additional amino acids, serine and arginine, between GFP and the amino terminus of the p60 protein. After confirming the entire sequence and reading frame, 5′GFP-p60pBlue was digested with XhoI and MluI to remove the insert; this fragment is named 5′GFP. 5′GFP was then ligated into pBCp60 (digested with XhoI and MluI) and transformed into TOP10 cells (Invitrogen); the resulting construct is named GFP-pBCp60. The plasmid insert was sequenced to confirm the GFP insertion and reading frame. All sequencing was performed using Big Dye Terminator 3.1 (Applied Biosystems) and analyzed on an ABI Prism 3100 Genetic Analyzer (Applied Biosystems).

For bacterial expression of wild-type and *pf19* p60, reverse transcription was performed using Superscript III (Invitrogen) using the p60-reverse primer and RNA isolated from wild-type or *pf19* cells as template. After two rounds of amplifications using nested primers (round 1: p69 forward to p60 reverse; round 2: p75 forward to p60 reverseN), the final PCR product was cloned into pCR2.1 (Invitrogen) and named p60cDNA-pCR. To express the cloned cDNA as a GST fusion, we engineered a BamHI site at the 5′ end of p60; p60cDNA-pCR was used as a template and amplified using M13forward and p60-BaM primers. The resulting product was cloned into pCR2.1 (p60Bam-pCR). The insert was removed from p60Bam-pCR by digestion with BamHI and EcoRI and ligated into pGex2T (GE Healthcare), thereby tagging p60 with GST at the 5′ end. The insert was sequenced for both wild-type and *pf19* clones to confirm reading frame and were then transformed into Rosetta Gami B (DE3) pLysS cells (Novagen) for expression.

### Transformation rescue

High efficiency transformation was achieved using the glass bead procedure of (Kindle, 1990). To test BAC clones and plasmids for rescue of mutant phenotypes, *pf19* cells were co-transformed with 1–3 μg of DNA and 1 μg of the *APHVIII* gene, conferring paromomycin resistance. Cells carrying integrated DNA were selected on 10 μg/ml paromomycin-TAP plates. Colonies were picked into TAP and screened for motility.

### amiRNA transformation and screening

Artificial microRNAi constructs were made according to Zhao and colleagues, and others (Zhao et al., 2009; Molnar et al., 2009; DiPetrillo and Smith, 2010) with the following modifications. The Web MicroRNA Designer (http://wmd3.weigelworld.org/cgi-bin/webapp.cgi (Ossowski et al., 2008) identified possible amiRNA sequences forp60 and designed forward and reverse oligonucleotides flanked by SpeI sites. Two amiRNA sequences were chosen that target p60 cDNA; no. 1: 5′-TAAGAAGGTGCACGATGTCTC-3′ targets nt961–980, no. 2: 5′-TTCAT-AGTACGTGTATCCCGC-3′ targets nt79–98. Annealed oligonucleotides were ligated into SpeI-digested pChlamiRNA3int plasmid, which contains the *APHVIII* gene. Colony PCR was used to screen bacterial transformants to confirm the correct orientation of the insert. Note regarding amiRNA in *Chlamydomonas*: the frequency with which we obtained knockdown of p60 expression = 1/704. We typically use two to three constructs for each gene of interest. The frequency of knockdown ranges from 0 per 2000 to 1 per 38 transformants (DiPetrillo and Smith, 2010; Dymek et al., 2011) and four other genes (unpublished data). The source of this variability is unknown. However, once knockdown of expression is achieved, the mutants are stable and exhibit no obvious off-target phenotypes.

### Southern blots

For each strain, 5 μg of genomic DNA was digested with KpnI and size fractionated on a 0.7% agarose gel. The DNA was transferred to MagnaGraph

nylon membrane (GE Healthcare) and UV crosslinked using the Stratagene Stratlinker. The membrane was probed with the *APHVIII*, *PF20, PF15* or *KAT1* genes which were each labeled with 50 μCi [α-$^{32}$P]dCTP using the Random Primed DNA Labeling Kit (Roche). The membrane was exposed to a phosphor screen and scanned with a Typhoon 9200 Imager (GE Healthcare).

#### Northern blots

Total RNA was isolated from cells at 0 minutes and 45 minutes post-deflagellation. Poly(A)$^+$ RNA was isolated from 1 mg of total RNA using the Oligotex mRNA Midi Kit (Qiagen). Poly(A)$^+$ RNA (10 μg) was fractionated on a 1% agarose gel containing formaldehyde and transferred to Hybond-N+ nylon membrane (GE Healthcare). The membrane was probed with wild-type p60cDNA which was labeled with 50 μCi of [α-$^{32}$P]dCTP using the Random Primed DNA Labeling Kit (Roche). The ribosomal *S14* gene was also labeled and used to probe the membrane as a loading control. The membrane was then exposed to a phosphor screen and scanned with a Typhoon 9200 Imager (GE Healthcare). Densitometry on the scanned image was performed with ImageJ (Rasband, W.S., ImageJ, US National Institutes of Health, Bethesda, Maryland, USA, http://rsb.info.nih.gov/ij/, 1997–2011). Relative expression levels were normalized using *S14* transcript levels. Northern blots were repeated for a minimum of three different experiments and we obtained consistent results.

#### Western blots

Axonemes were isolated as described previously (Dymek and Smith, 2007). Axonemes (10 μg) or whole cells ($1\times10^6$ cells) were resolved by SDS-PAGE using a 7% polyacrylamide gel. Following electrophoresis, the samples were transferred to PDVF membrane (Millipore). Membranes were blocked in 5% milk in TBST for 1 hour at room temperature and then incubated with primary antibody diluted in TBST for two hours at room temperature [anti-PF20 1:10,000, affinity purified anti-CaM-IP3 1:1000, anti-RSP1 (generously provided by Joel Rosenbaum, Yale University) 1:10,000, anti-GFP290 (AbCam) 1:1000, anti-p60 serum (generously provided by Lynne Quarmby, Simon Fraser University) 1:1000 or affinity purified anti-p60 (generously provided by Lynne Quarmby) 1:500]. Blots were washed and incubated with secondary antibody diluted in TBST for 30 minutes at room temperature [anti-rabbit-HRP (GE Healthcare) 1:30,000 or anti-mouse-HRP (Thermo Scientific) 1:10,000]. Blots were washed and developed using the ECL Plus Western Blotting Detection System (GE Healthcare).

#### Assay for cell growth

A loopful of cells was resuspended in 1 ml TAP medium and counted with a hemocytometer. An equal number of cells ($9.4\times10^7$ cells) were added to 250 ml TAP bubblers ($3.76\times10^5$ cells/ml). Cells were bubbled in constant light for 3 days. At 24, 48, and 72 hours, samples were collected and counted using a hemocytometer. The results were plotted in MS-Excel.

#### Electron microscopy and central pair counts

For analysis of flagellar defects, axonemes from WT and mutants of interest were prepared for thin-section electron microscopy. Specimens were fixed with 1% glutaraldehyde and 1% tannic acidin 0.1 M sodium cacodylate, postfixed in 1% osmium tetroxide, dehydrated in a graded series of ethanol, and embedded in LX112 resin. Uniform silver-gray sections were mounted on Formvar-coated, carbon-stabilized copper grids, stained with uranyl acetate and Reynolds lead citrate, and examined at 100 kV in a transmission electron microscope (JOEL JEM-1010). To quantify central pair defects, transverse sections of axonemes were classified as having two, one or no central microtubules present. Axonemes with electron dense material were considered a separate category.

#### Protein expression and microtubule severing assay

Wild-type and *pf19* p60cDNA in the pGex2T plasmid were transformed into Rosetta Gami B (DE3) pLysS cells (Novagen) and grown to an $OD_{600}$ of 0.6 at 37℃, then induced overnight at 30℃ with 1 mM IPTG. Wild-type or *pf19* p60-GST was purified using GST-Bind resin using non-denaturing conditions according to the manufacturer's methods (Novagen). Protein concentration was determined spectrophotometrically. Protein in peak fractions was resolved by SDS-PAGE using a 7% polyacrylamide gel and visualized by Coomassie Blue staining. For microtubule severing assays, ATP was added to a final concentration of 1 mM to both wild-type and *pf19* p60–GST peak fractions. Microtubules were polymerized in vitro (Cytoskeleton) and resuspended to a concentration of 0.25 mg/ml in NaLow (10 mM Hepes, 5 mM $MgSO_4$, 1 mM DTT, 0.5 mM EDTA, and 30 mM NaCl, pH 7.5). Flow chambers were made on microscope slides coated with poly-lysine (1:600, Sigma) using double stick tape with coverlips placed on top. Microtubules (10 μl) were pipetted into the chamber and rinsed with 40 μl of NaLow. Then 40 μl (~10 μg) of WT p60–GST, pf19 p60–GST or NaLow was flowed through the chamber, followed by 40 μl of WT p60–GST+ATP, pf19 p60–GST+ATP or NaLow+ATP (1 mM ATP). For all samples, 40 μl of NaLow/ATP was then flowed through the chamber. Images were observed on an Axioskope 2 microscope (Zeiss, Inc.) equipped for dark-field optics including a Plan-Apochromate 40× oil immersion objective with iris and ultra dark-field oil immersion condenser. Images were captured at 0 and 20 minutes using a silicon-intensified target camera (VE-1000 SIT; Dage-MTI, Inc.) and converted to digital images using Labview 7.1 software (National Instruments, Austin, TX). Image J (Rasband, W.S., ImageJ, US National–Institutes of Health, Bethesda, Maryland, USA, http://rsb.info.nih.gov/ij/, 1997–2011) was used to quantify the amount of microtubules in each image. For each set of 0- and 20-minute images, the threshold levels were set to differentiate microtubules from background and then equalized between the two images. Mean grey values were then measured and compared between corresponding sets of 0- and 20-minute time points. In all cases the mean grey value decreased after 20 minutes. The difference in mean grey value is expressed as a percent decrease. For each experimental group, at least 10 image sets were analyzed.

#### Immunofluorescence microscopy

Immunofluorescence was performed according to Dymek and colleagues (Dymek et al., 2006). Briefly, dividing cells were adhered to poly-lysine-coated coverslips, fixed with methanol for 15 minutes and allowed to dry for 15 minutes. Coverslips were blocked for 1 hr in 5% BSA/PBS and incubated overnight in anti-acetylated α-tubulin antibodies (Sigma; clone 611B1, 1:100 in 1% BSA/PBS). Coverslips were washed with PBS and incubated for 1 hour in anti-mouse (Texas Red) secondary antibody (Vector Labs, 1:500 in 1% BSA/PBS) and washed with PBS. Coverslips were placed on microscope slides with a drop of prolong anti-fade (Invitrogen) and allowed to dry overnight in the dark.

## Acknowledgements

The authors are grateful for expert technical support for this work from Natalie Vajda, and thank Pete Lefebvre, Win Sale and Roger Sloboda for critically reading the manuscript.

## Funding

This work was supported by National Institutes of Health [grant number GM066919 to E.F.S.]. Deposited in PMC for release after 12 months.

Supplementary material available online at
http://jcs.biologists.org/lookup/suppl/doi:10.1242/jcs.096941/-/DC1

## References

**Adams, G. M., Huang, B., Piperno, G. and Luck, D. J.** (1981). Central-pair microtubular complex of Chlamydomonas flagella: polypeptide composition as revealed by analysis of mutants. *J. Cell Biol.* **91**, 69-76.

**Ahmad, F. J., Yu, W., McNally, F. J. and Baas, P. W.** (1999). An essential role for katanin in severing microtubules in the neuron. *J. Cell Biol.* **145**, 305-315.

**Baas, P. W. and Sudo, H.** (2010). More microtubule severing proteins: more microtubules. *Cell Cycle* **9**, 2271-2274.

**Bichet, A., Desnos, T., Turner, S., Grandjean, O. and Höfte, H.** (2001). BOTERO1 is required for normal orientation of cortical microtubules and anisotropic cell expansion in Arabidopsis. *Plant J.* **25**, 137-148.

**Bouquin, T., Mattsson, O., Naested, H., Foster, R. and Mundy, J.** (2003). The Arabidopsis lue1 mutant defines a katanin p60 ortholog involved in hormonal control of microtubule orientation during cell growth. *J. Cell Sci.* **116**, 791-801.

**Burk, D. H., Liu, B., Zhong, R., Morrison, W. H. and Ye, Z. H.** (2001). A katanin-like protein regulates normal cell wall biosynthesis and cell elongation. *Plant Cell* **13**, 807-827.

**Casanova, M., Crobu, L., Blaineau, C., Bourgeois, N., Bastien, P. and Pagès, M.** (2009). Microtubule-severing proteins are involved in flagellar length control and mitosis in Trypanosomatids. *Mol. Microbiol.* **71**, 1353-1370.

**Díaz-Valencia, J. D., Morelli, M. M., Bailey, M., Zhang, D., Sharp, D. J. and Ross, J. L.** (2011). Drosophila katanin-60 depolymerizes and severs at microtubule defects. *Biophys. J.* **100**, 2440-2449.

**DiPetrillo, C. G. and Smith, E. F.** (2010). Pcdp1 is a central apparatus protein that binds Ca(2+)-calmodulin and regulates ciliary motility. *J. Cell Biol.* **189**, 601-612.

**Dutcher, S. K., Huang, B. and Luck, D. J.** (1984). Genetic dissection of the central pair microtubules of the flagella of Chlamydomonas reinhardtii. *J. Cell Biol.* **98**, 229-236.

**Dymek, E. E. and Smith, E. F.** (2007). A conserved CaM- and radial spoke associated complex mediates regulation of flagellar dynein activity. *J. Cell Biol.* **179**, 515-526.

**Dymek, E. E., Lefebvre, P. A. and Smith, E. F.** (2004). PF15p is the chlamydomonas homologue of the Katanin p80 subunit and is required for assembly of flagellar central microtubules. *Eukaryot. Cell* **3**, 870-879.

**Dymek, E. E., Goduti, D., Kramer, T. and Smith, E. F.** (2006). A kinesin-like calmodulin-binding protein in Chlamydomonas: evidence for a role in cell division and flagellar functions. *J. Cell Sci.* **119**, 3107-3116.

**Dymek, E. E., Heuser, T., Nicastro, D. and Smith, E. F.** (2011). The CSC is required for complete radial spoke assembly and wild-type ciliary motility. *Mol. Biol. Cell* **22**, 2520-2531.

**Gaertig, J. and Wloga, D.** (2008). Ciliary tubulin and its post-translational modifications. *Curr. Top. Dev. Biol.* **85**, 83-113.
**Gardiner, J. and Marc, J.** (2011). Arabidopsis thaliana, a plant model organism for the neuronal microtubule cytoskeleton? *J. Exp. Bot.* **62**, 89-97.
**Gorman, D. S. and Levine, R. P.** (1965). Cytochrome f and plastocyanin: their sequence in the photosynthetic electron transport chain of Chlamydomonas reinhardi. *Proc. Natl. Acad. Sci. USA* **54**, 1665-1669.
**Hartman, J. J. and Vale, R. D.** (1999). Microtubule disassembly by ATP-dependent oligomerization of the AAA enzyme katanin. *Science* **286**, 782-785.
**Hartman, J. J., Mahr, J., McNally, K., Okawa, K., Iwamatsu, A., Thomas, S., Cheesman, S., Heuser, J., Vale, R. D. and McNally, F. J.** (1998). Katanin, a microtubule-severing protein, is a novel AAA ATPase that targets to the centrosome using a WD40-containing subunit. *Cell* **93**, 277-287.
**Karabay, A., Yu, W., Solowska, J. M., Baird, D. H. and Baas, P. W.** (2004). Axonal growth is sensitive to the levels of katanin, a protein that severs microtubules. *J. Neurosci.* **24**, 5778-5788.
**Kathir, P., LaVoie, M., Brazelton, W. J., Haas, N. A., Lefebvre, P. A. and Silflow, C. D.** (2003). Molecular map of the Chlamydomonas reinhardtii nuclear genome. *Eukaryot. Cell* **2**, 362-379.
**Kindle, K. L.** (1990). High-frequency nuclear transformation of Chlamydomonas reinhardtii. *Proc. Natl. Acad. Sci. USA* **87**, 1228-1232.
**Lechtreck, K. F. and Witman, G. B.** (2007). Chlamydomonas reinhardtii hydin is a central pair protein required for flagellar motility. *J. Cell Biol.* **176**, 473-482.
**Lohret, T. A., McNally, F. J. and Quarmby, L. M.** (1998). A role for katanin-mediated axonemal severing during Chlamydomonas deflagellation. *Mol. Biol. Cell* **9**, 1195-1207.
**Lohret, T. A., Zhao, L. and Quarmby, L. M.** (1999). Cloning of Chlamydomonas p60 katanin and localization to the site of outer doublet severing during deflagellation. *Cell Motil. Cytoskeleton* **43**, 221-231.
**Loughlin, R., Wilbur, J. D., McNally, F. J., Nédélec, F. J. and Heald, R.** (2011). Katanin contributes to interspecies spindle length scaling in Xenopus. *Cell* **147**, 1397-1407.
**Mains, P. E., Kemphues, K. J., Sprunger, S. A., Sulston, I. A. and Wood, W. B.** (1990). Mutations affecting the meiotic and mitotic divisions of the early Caenorhabditis elegans embryo. *Genetics* **126**, 593-605.
**McKean, P. G., Baines, A., Vaughan, S. and Gull, K.** (2003). Gamma-tubulin functions in the nucleation of a discrete subset of microtubules in the eukaryotic flagellum. *Curr. Biol.* **13**, 598-602.
**McNally, F. J. and Vale, R. D.** (1993). Identification of katanin, an ATPase that severs and disassembles stable microtubules. *Cell* **75**, 419-429.
**McNally, K. P. and McNally, F. J.** (2011). The spindle assembly function of Caenorhabditis elegans katanin does not require microtubule-severing activity. *Mol. Biol. Cell* **22**, 1550-1560.
**McNally, K. P., Bazirgan, O. A. and McNally, F. J.** (2000). Two domains of p80 katanin regulate microtubule severing and spindle pole targeting by p60 katanin. *J. Cell Sci.* **113**, 1623-1633.
**Mitchell, D. R. and Sale, W. S.** (1999). Characterization of a Chlamydomonas insertional mutant that disrupts flagellar central pair microtubule-associated structures. *J. Cell Biol.* **144**, 293-304.
**Molnar, A., Bassett, A., Thuenemann, E., Schwach, F., Karkare, S., Ossowski, S., Weigel, D. and Baulcombe, D.** (2009). Highly specific gene silencing by artificial microRNAs in the unicellular alga Chlamydomonas reinhardtii. *Plant J.* **58**, 165-174.
**Nagawa, S., Sawa, S., Sato, S., Kato, T., Tabata, S. and Fukuda, H.** (2006). Gene trapping in Arabidopsis reveals genes involved in vascular development. *Plant Cell Physiol.* **47**, 1394-1405.
**Nakamura, M., Ehrhardt, D. W. and Hashimoto, T.** (2010). Microtubule and katanin-dependent dynamics of microtubule nucleation complexes in the acentrosomal Arabidopsis cortical array. *Nat. Cell Biol.* **12**, 1064-1070.
**Ossowski, S., Schwab, R. and Weigel, D.** (2008). Gene silencing in plants using artificial microRNAs and other small RNAs. *Plant J.* **53**, 674-690.
**Parker, J. D., Hilton, L. K., Diener, D. R., Rasi, M. Q., Mahjoub, M. R., Rosenbaum, J. L. and Quarmby, L. M.** (2010). Centrioles are freed from cilia by severing prior to mitosis. *Cytoskeleton* **67**, 425-430.
**Rasi, M. Q., Parker, J. D., Feldman, J. L., Marshall, W. F. and Quarmby, L. M.** (2009). Katanin knockdown supports a role for microtubule severing in release of basal bodies before mitosis in Chlamydomonas. *Mol. Biol. Cell* **20**, 379-388.
**Roll-Mecak, A. and McNally, F. J.** (2010). Microtubule-severing enzymes. *Curr. Opin. Cell Biol.* **22**, 96-103.
**Sanders, M. A. and Salisbury, J. L.** (1994). Centrin plays an essential role in microtubule severing during flagellar excision in Chlamydomonas reinhardtii. *J. Cell Biol.* **124**, 795-805.
**Sharma, N., Bryant, J., Wloga, D., Donaldson, R., Davis, R. C., Jerka-Dziadosz, M. and Gaertig, J.** (2007). Katanin regulates dynamics of microtubules and biogenesis of motile cilia. *J. Cell Biol.* **178**, 1065-1079.
**Silflow, C. D., Liu, B., LaVoie, M., Richardson, E. A. and Palevitz, B. A.** (1999). Gamma-tubulin in Chlamydomonas: characterization of the gene and localization of the gene product in cells. *Cell Motil. Cytoskeleton* **42**, 285-297.
**Smith, E. F. and Lefebvre, P. A.** (1996). PF16 encodes a protein with armadillo repeats and localizes to a single microtubule of the central apparatus in Chlamydomonas flagella. *J. Cell Biol.* **132**, 359-370.
**Smith, E. F. and Lefebvre, P. A.** (1997). PF20 gene product contains WD repeats and localizes to the intermicrotubule bridges in Chlamydomonas flagella. *Mol. Biol. Cell* **8**, 455-467.
**Smith, E. F. and Lefebvre, P. A.** (2000). Defining functional domains within PF16: a central apparatus component required for flagellar motility. *Cell Motil. Cytoskeleton* **46**, 157-165.
**Stoppin-Mellet, V., Gaillard, J. and Vantard, M.** (2002). Functional evidence for in vitro microtubule severing by the plant katanin homologue. *Biochem. J.* **365**, 337-342.
**Stoppin-Mellet, V., Gaillard, J. and Vantard, M.** (2003). Plant katanin, a microtubule severing protein. *Cell Biol. Int.* **27**, 279.
**Stoppin-Mellet, V., Gaillard, J., Timmers, T., Neumann, E., Conway, J. and Vantard, M.** (2007). Arabidopsis katanin binds microtubules using a multimeric microtubule-binding domain. *Plant Physiol. Biochem.* **45**, 867-877.
**Sudo, H. and Baas, P. W.** (2010). Acetylation of microtubules influences their sensitivity to severing by katanin in neurons and fibroblasts. *J. Neurosci.* **30**, 7215-7226.
**Tam, L. W. and Lefebvre, P. A.** (1993). Cloning of flagellar genes in Chlamydomonas reinhardtii by DNA insertional mutagenesis. *Genetics* **135**, 375-384.
**Wasteneys, G. O.** (2002). Microtubule organization in the green kingdom: chaos or self-order? *J. Cell Sci.* **115**, 1345-1354.
**Webb, M., Jouannic, S., Foreman, J., Linstead, P. and Dolan, L.** (2002). Cell specification in the Arabidopsis root epidermis requires the activity of ECTOPIC ROOT HAIR 3--a katanin-p60 protein. *Development* **129**, 123-131.
**Yu, W., Solowska, J. M., Qiang, L., Karabay, A., Baird, D. and Baas, P. W.** (2005). Regulation of microtubule severing by katanin subunits during neuronal development. *J. Neurosci.* **25**, 5573-5583.
**Yu, W., Qiang, L., Solowska, J. M., Karabay, A., Korulu, S. and Baas, P. W.** (2008). The microtubule-severing proteins spastin and katanin participate differently in the formation of axonal branches. *Mol. Biol. Cell* **19**, 1485-1498.
**Zhang, D., Grode, K. D., Stewman, S. F., Diaz-Valencia, J. D., Liebling, E., Rath, U., Riera, T., Currie, J. D., Buster, D. W., Asenjo, A. B. et al.** (2011). Drosophila katanin is a microtubule depolymerase that regulates cortical-microtubule plus-end interactions and cell migration. *Nat. Cell Biol.* **13**, 361-369.
**Zhao, T., Wang, W., Bai, X. and Qi, Y.** (2009). Gene silencing by artificial microRNAs in Chlamydomonas. *Plant J.* **58**, 157-164.

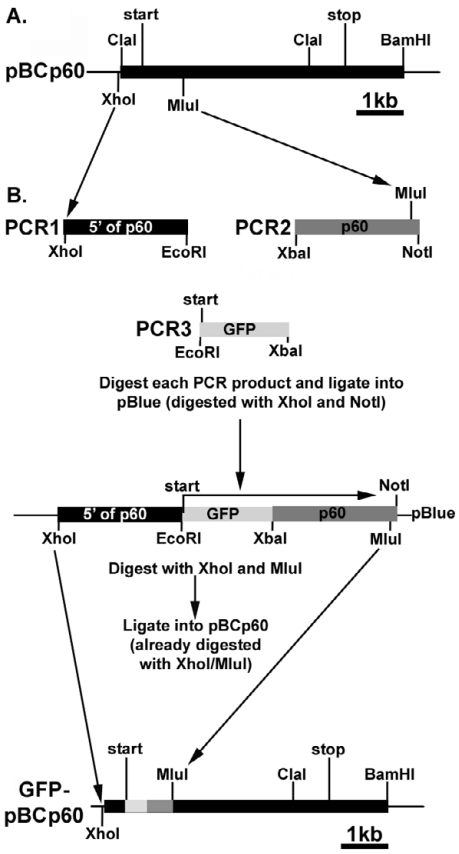


**Fig. S1. Diagram of p60 clones.** (**A**) Illustration of the p60 subclone obtained from clone 27D3 in the *Chlamydomonas* BAC library. The translational start and stop sites are indicated. (**B**) Diagram of cloning strategy for generating p60-GFP. Essentially, the 5′ end of the KAT1 gene was subcloned to engineer convenient restriction sites for adding the gene encoding GFP immediately downstream of the translational start site. See materials and Methods for details.

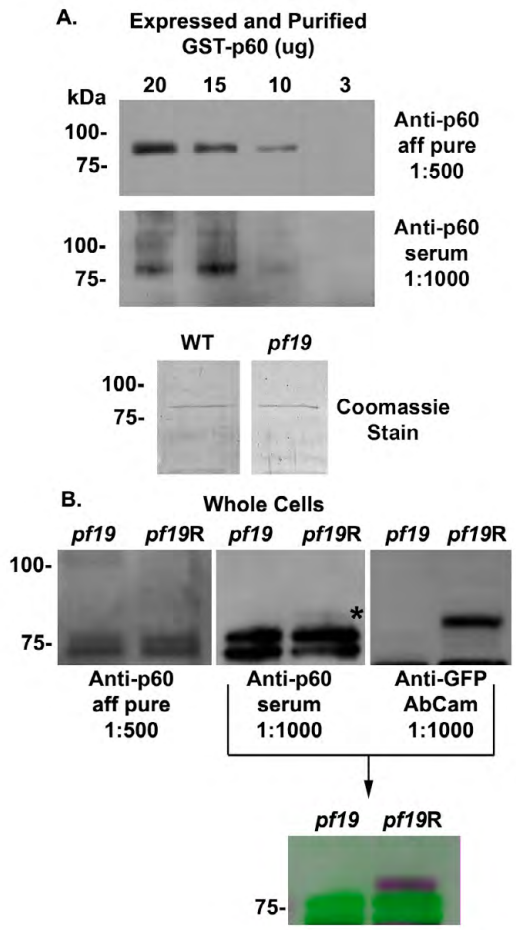


**Fig. S2. Anti-p60 western blots.** (**A**) Top panels are western blots of bacterially expressed and purified WT p60-GST. Serum and affinity purified antibodies were obtained from the Quarmby Lab (Simon Fraser University). Both the affinity pure p60 antibody and the p60 serum recognize a band of the correct size for p60-GST (~85 kDa). The lower limit of detection is 10 µg of purified protein for both. Lower panels in A are Coomassie stained gels of purified bacterially expressed WT and pf19 p60-GST demonstrating purity of p60 used for microtubule severing assays. (**B**) Whole cell western blots of pf19 and pf19R (pf19 transformed with GFP-pBCp60). 106 cells were loaded into each lane. Anti-GFP antibodies recognize one band at ~85 kDa in the pf19R lane, the expected size of GFPp60. Affinity pure p60 antibodies and serum recognize doublet bands at 75 kDa in pf19 and pf19R. Since the serum was unable to detect less than 10 µg of pure p60 protein, a far greater amount of protein than is present in our western blots of cell extracts, it is unlikely that the doublet is p60. The anti-GFP blot was reprobed with anti-p60 serum in order to directly overlay the two images (bottom image). The asterisk in the anti-p60 serum blot denotes signal from the anti-GFP probe. Using Adobe Photoshop, the image of the anti-GFP reactive band was colored magenta and the image of the anti-p60 reactive bands was colored green. Images were made semi-transparent and overlayed; since the images were produced from the same blot, they were aligned using the molecular weight markers. Any overlap in magenta and green should appear as white. No white overlay is observed between the two images. In addition, the magenta GFP band is of larger molecular weight than the green doublet band. Therefore, neither the affinity pure antibody nor the anti-p60 serum from the p60 antibodies recognizes the p60-GFP protein in pf19R cells.

| Name | Primer Sequence 5'-3' |
|---|---|
| **Primers for obtaining p60 cDNA** | |
| P69for | CAAGCGCCGTTGACATGTG |
| P60rev | GTTGTGTCACGCCAAGTGTG |
| P75for | GACATACTGCGACTAGCGTG |
| P60RevN | CTTACTGGCATGACACCGTTAC |
| **Primers for generating p60-GFP** | |
| P60Xho | CCGCTCGAGGTTTAGCGCATTTATGTAG |
| P60NEco | CTTGAATTCCTCCACGCACGCGCCTCAAGTTG |
| P60NXba | GAAATCTAGAGGGGGCGCGGACGTGCAG |
| P60MluNotI | GATGCGGCCGCCAAAAAGTATTCAACGCGTAC |
| P60Bam | GATAGGATCCGCGGACGTGCAGGCGATC |
| P60GFPNEco | GTTGAATTCATGGCCAAGGGCGAGGAG |
| P60GFPXba | CGTTCTAGACTTGTACAGCTCGTCCATG |
| **Primers for amiRNA** | |
| **Construct 1** | |
| **For1** | CTAGTGAGACATCGTGCACCTACTTATCTCGCTGATCGGCACCATGGGG GTGGTGGTGATCAGCGCTATAAGAAGGTGCACGATGTCTCG |
| **Rev1** | CTAGCGAGACATCGTGCACCTTCTTATAGCGCTGATCACCACCACCCCC ATGGTGCCGATCAGCGAGATAAGTAGGTGCACGATGTCTCA |
| **Construct 2** | |
| **For2** | CTAGTGCGGGATACACGTACTTTGAATCTCGCTGATCGGCACCATGGGG GTGGTGGTGATCAGCGCTATTCATAGTACGTGTATCCCGCG |
| **Rev2** | CTAGCGCGGGATACACGTACTATGAATAGCGCTGATCACCACCACCCCC ATGGTGCCGATCAGCGAGATTCAAAGTACGTGTATCCCGCA |

**Table S1. Primers used in this study**